Modeling the Thermal Response of Porcine Cartilage to Laser Irradiation

Sergio H. Díaz [a], Guillermo Aguilar [a,b], Reshmi Basu [a], Enrique Lavernia [c], and Brian J. F. Wong [a]
[a]Beckman Laser Institute, Univ. of California, Irvine, CA 92612
[b]Center for Biomedical Engineering, Univ. of California, Irvine, CA 92697
[c]Deptartment of Chemical Engineering and Material Sciences., Univ of California, Irvine, CA 92697

ABSTRACT

Cartilage laser thermoforming, also known as laser reshaping, is a new surgical procedure that allows *in-situ* treatment of deformities in the head and neck with less morbidity than traditional approaches. During laser irradiation, cartilage becomes sufficiently subtle or deformable for stretching and shaping into new stable configurations. This study describes the experimental and theoretical characterization of the thermal response of porcine cartilage to laser irradiation (Nd:YAG). The surface temperature history of cartilage specimens was monitored during heating and thermal relaxation; using laser exposure times ranging between 1 and 15 s and laser powers of 1 to 10 W. The experimental results were then used to validate a finite element model, which accounts for heat diffusion, light propagation in tissue, and heat loss due to water evaporation. The simultaneous solution of the energy and mass diffusion equations resulted in predictions of temperature distribution in cartilage that were in good agreement with experiments. The model simulations will provide insights to the relationship between the laser treatment parameters (exposure time, laser beam diameter, and power) and the onset of new molecular arrangements and cell thermal injury in the material, thus conceiving basic guidelines of laser thermoforming.

Keywords: Cartilage reshaping, finite element modeling, laser beam profile, Monte Carlo, plastic surgery, stress relaxation, tissue damage.

1. INTRODUCTION

Laser assisted reshaping of cartilage is a new surgical procedure designed to allow *in-situ* treatment of deformities in the head and neck with less morbidity than traditional approaches [1]. During laser irradiation, mechanically deformed cartilage undergoes accelerated stress relaxation that permits tissue to be reshaped into new stable configurations. The principal advantage of using laser radiation to generate thermal energy in tissue is the precise control of the space-time dependent temperature distribution.

Optimization of the reshaping process requires characterization of the temperature-dependent stress relaxation and correlation of these changes with observed alterations in cartilage physical properties (e.g., elastic modulus, thermal diffusivity, and optical scattering). While animal and human studies have demonstrated clinical feasibility [2,3] the fundamental biophysical mechanisms accompanying laser reshaping are largely unknown. It has been suggested that the mechanism responsible for laser reshaping is primarily associated with the release of cartilaginous bound water to free water taking place at a temperature of about $T_w \cong 65$ °C [4]. Along with this molecular reorganization, protein denaturation and subsequent cell death can take place at this temperature. Therefore, cartilage specimens must be heated to the critical transition temperature for reshaping, while maintaining temperature and laser exposure to a minimum to reduce cellular injury.

This sensitive balance between permanent shape change and cell viability requires the accurate prediction of the temperature distribution during laser irradiation. The purpose of this study was to develop a finite element model (FEM) able to predict the temperature distribution in a slab of porcine nasal cartilage during laser irradiation. This model incorporates heat diffusion, light propagation in tissue, and water evaporation from the surfaces of the slab. Numerical results were compared to the experimental characterization of the thermal distribution in cartilage during Nd:YAG laser (λ = 1.32 μm) irradiation, where surface temperature of the specimen was measured with a non-contact (infrared emission) probe.

Laser Tissue Interaction XIII: Photochemical, Photothermal, and Photomechanical, Steven L. Jacques, Donald D. Duncan, Sean J. Kirkpatrick, Andres Kriete, Editors, Proceedings of SPIE Vol. 4617 (2002)

2. THE HEAT EQUATION

The temperature response of tissue to laser irradiation is governed by the following equation,

$$\rho c \frac{\partial T}{\partial t} = \kappa \frac{\partial^2 T}{\partial z^2} + Q_i \tag{1}$$

where T is temperature (K), ρ density (Kg/m^3), c the specific heat (J/kg K) of the tissue, κ the thermal conductivity (W/m K), and Q_i the rate of internal heating due to irradiation. Transformation of light into thermal energy depends on the light fluence rate distribution, $\phi(r,z)$ (W/m^2) and absorption coefficient, μ_a (m^{-1}) of the tissue, given by

$$Q_i = \mu_a \phi(r,z) \tag{2}$$

The $\phi(r,z)$ can be estimated as a function of penetration depth in tissue using various light distribution models [5]. In this work, $\phi(r,z)$ is estimated using a Monte Carlo algorithm developed by Wang et al.[6,7], where the specimen thickness, tissue optical properties, and laser beam power and diameter are used as input parameters to the code.

Water loss due to evaporation was also considered in the finite element model. Evaporation occurs from the cartilage surface and the energy associated with the phase change is the latent heat of liquid vaporization. The energy required to sustain evaporation, Q_{vap}, must come from the internal energy of the liquid (free water in cartilage), which then experiences a reduction in temperature [8]. Q_{vap} may be approximated as the product of evaporative mass flux and latent heat of vaporization [8], as

$$Q_{vap} = n''_{vap}\, h_{fg} \tag{3}$$

where h_{fg} is the phase change enthalpy (J/kg). The mass flux n''_{vap} (Kg/s m^2) of water vapor may be expressed as

$$n''_{vap} = h_m [\rho_{vap,sat}(T_s) - \rho_{vap,\infty}] \tag{4}$$

or as a mass transfer rate n_{vap} (Kg/s) given by

$$n_{vap} = h_m A_s [\rho_{vap,sat}(T_s) - \rho_{vap,\infty}] \tag{5}$$

where h_m is the convection mass transfer coefficient (m/s), $\rho_{vap,sat}(T_s)$ the density of saturated water vapor (kg/m^3) at the surface temperature (T_s) of the tissue (which can be obtained from thermodynamic tables of water), $\rho_{vap,\infty}$ the density of water vapor in air (kg/m^3) at room temperature, and A_s the exposed surface area (m^2). The $\rho_{vap,\infty}$ can be estimated from the relative humidity, Rh, as

$$Rh = \frac{P_v}{P_g} = \frac{\rho_{vap,\infty}}{\rho_{vap,sat}(T_\infty)} \tag{6}$$

where P_v is the partial pressure of vapor as it exists in the water vapor-air mixture, and P_g the saturation vapor pressure at the same temperature.

3. THE FINITE ELEMENT MODEL (FEM)

Problems involving time-dependent thermal and optical properties, irregular boundary conditions, or complex geometries are very often difficult to formulate using analytical solutions. These problems can be solved by numerical methods, such as the finite difference method or the finite element method. A numerical time-dependent solution of the heat equation has been obtained using a finite element code (FEMBLAB®, Comsol Inc., Burlington, MA) in order to calculate spatial and temporal temperature profiles, $T(r,z,t)$ of irradiated tissue.

The FEM consists of approximately 230 nodes and 400 elements. An axi-symmetric model was used to simulate laser irradiation of a cylinder of cartilage of semi-infinite radius and finite thickness, as shown in Figure 1. The following thermal properties of cartilage (measured or assumed to be equal to those of water) were used in the numerical analysis: ρ = 1.26 Kg/cm^3, c = 4.0 J/Kg K, κ = 0.6 W/m K. The tissue initial temperature (T_o) varied between 18-20 °C, room temperature (T_∞) ranged between 22-23 °C. The thermal boundary condition at an air-tissue interface, top, bottom, and perimeter (r_{inf} = 10 mm) surfaces, accounted for convective heat loss (free convection) and water vaporization. The applied laser powers ranged from 1-10 W and irradiation times varied between 1-15 seconds. Laser spot radius (r_o) was 2.5 mm. Values of specimen thickness (D) ranged between 1 and 4 mm.

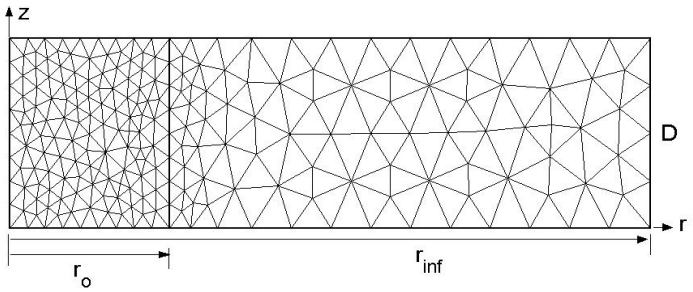

Figure 1. Axi-symmetric model of cartilage specimen.

4. MATERIALS AND METHODS

4.1 Tissue preparation

Fresh cartilage specimens from domestic pigs were obtained from a local packing house (Farmers John, Vernon,CA) and harvested as described by Wong et al. [9]. Several cartilage grafts from each septal cartilage were obtained and sectioned into rectangular slabs measuring 25 mm x 30 mm with thickness of 1 to 4 mm. Uniform specimen thickness was accomplished by removing the outermost layers of the intact full-thickness septal cartilage using a commercial rotary food slicer (model 620, Chef's Choice Int., EdgeCraft Corp, Avondale, PA) until the desired thickness was reached [10]. Specimens were then kept in saline solution until testing.

4.2 Temperature measurement

Cartilage specimens were irradiated during 1-15 s using Nd:YAG laser (λ = 1.32 μm, 50 Hz PRR, Laser Aesthetics, Auburn, CA) using several laser powers (1–10 W). Laser energy was delivered using a 400-μm core-diameter silica multimode optical fiber terminating in a collimating lens. Laser spot size (2.5 mm radius) and power were measured with thermal paper and a pyroelectric meter (Model 200/10, Coherent, Auburn CA), respectively.

Surface temperature (T_s) was measured using an infrared emission sensor (response time of 120 ms (95%), spectral sensitivity 7.6-18 μm, Laser Aesthetics), and calibrated using a hot/cold blackbody calibration source (Model BB701, Omega Engineering Inc., Stamford, CT) set at different known temperatures. An analog to digital converter (AT-MIO-16XE-50, National Instruments, Austin, TX) was used to record T_s using software written in LabVIEW (National Instruments) running on a personal computer (AMD, 750 MHz).

4.3 Laser beam profile measurement

The laser beam intensity profile was measured by repeatedly irradiating the tip of a thermocouple at different locations across the beam diameter, as described in [11]. At each location, x, the maximum temperature change, $\Delta T_{max}(x)$, measured by the sensor was assumed to be proportional to the spatial distribution of the beam intensity. The profile was obtained from the $\Delta T_{max}(x)$ plot, as shown in Figure 2. The temperature change measured at each location was normalized with respect to the average temperature change recorded at points near the approximate center of the laser beam ($-1 < x < 1$ mm). The beam radius was defined as the location x where the laser beam intensity decays to 50% of its maximum value, indicated by dashed lines in Figure 2. The resultant beam radius, r = 2.5 mm, agreed well with the direct measurement of beam radius obtained using thermal paper.

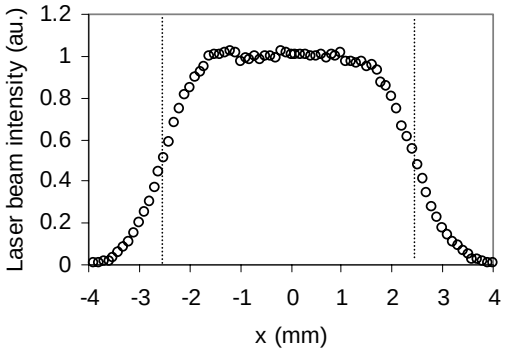

Figure 2. Spatial distribution of the laser beam intensity. Dashed lines indicate locations where intensity decays to 50% of its maximum value.

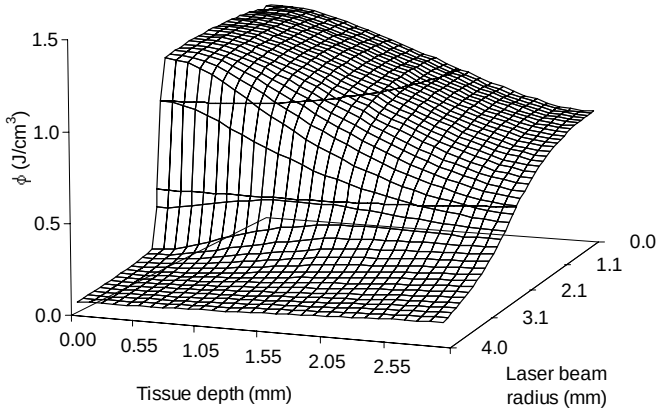

Figure 3. Fluence rate distribution versus tissue depth and laser beam radius in a 3mm thick slab of cartilage relative to a radiant exposure of 1 J/cm^2.

4.4 Fluence rate calculation.

Laser irradiation of tissue transforms into thermal energy deposition. The efficacy of this transformation depends on the laser wavelength and optical properties of the tissue involved. Optical properties of porcine cartilage at a wavelength of 1.32 μm are characterized by low absorption, μ_a = 100 m^{-1}, high scattering $\mu_s' = \mu_s(1\text{-}g)$ = 260 m^{-1}, and mean cosine of the scattering angle $g \approx 0.9$ [12]. Tissue index of refraction, n, was assumed to be 1.37. Figure 3 illustrates the fluence rate distribution in a 3 mm thick cartilage specimen as a function of tissue depth and radius, estimated using the Multi-Layer Monte Carlo (MLMC) and Convolution (CONV) codes [6,7]. A flat laser beam profile of 2.5 mm in radius and a unitary irradiance of 1 J/cm^2 were used as input parameters to the Monte Carlo simulation.

In addition to wavelength and optical properties, $\phi(r,z)$ depends on the laser beam characteristics and thickness D of the irradiated specimen. In our calculations, only the latter changed since the tissue optical properties were considered constant in the temperature range of interest (20-80 °C) and the laser beam profile was measured and remained unchanged. Figure 4 shows curves of $\phi(z)$ as a function of tissue depth, calculated at the center of the laser beam for three different thicknesses of cartilage.

4.5 Mass transfer rate measurement

A first estimation of the mass transfer coefficient h_m involved in the evaporative cooling was indirectly obtained by measuring the mass transfer rate n_{vap} of water in cartilage to the atmosphere. A rectangular slab of cartilage (52 x 18 x 2 mm) was left to dry at room temperature for 10 min on top of a microbalance (Model R200D, SY Nielson Service Inc., Riverside CA). The mass transfer rate was estimated from the slope of the weight vs. time plot, shown in Figure 5. The experiment was repeated using the same specimen following a period (10 min) of re-hydration in saline solution. From this graph n_{vap} is found to be ≈ 7E-8 (kg/s).

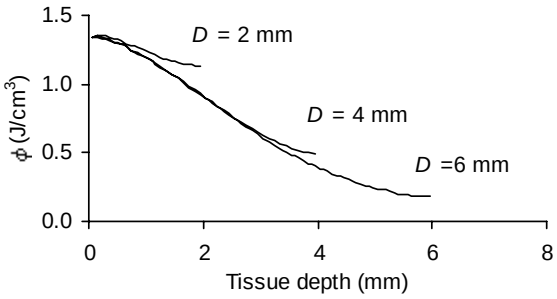

Figure 4. Predicted $\phi(z)$ as a function of tissue depth at the center of the laser beam. Calculations for specimen thickness of 2,4 and 6 mm.

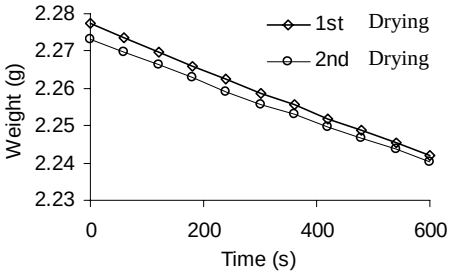

Figure 5. Mass transfer rate of water in cartilage due to evaporation.

A second experiment was designed to measure the transient and steady-state temperatures of cartilage during the evaporative cooling process. A thermocouple was inserted into the center of a square slab of cartilage (15x15x3 mm). The specimen was initially kept in saline solution at 20 °C. Subsequently, the specimen was taken out of the solution, excess superficial water was removed, and left to dry at room temperature until thermal equilibrium was reached.

Figure 6 illustrates the temperature-time plot, showing a steady-state temperature of the cartilage specimen, T_{cart} ≅16°C at time t > 500 s. This equilibrium temperature is in fact equivalent to the so-called wet bulb temperature, which can be obtained from a psychrometric chart knowing the room temperature (T_∞ = 23 °C) and relative humidity (Rh = 50%). Finally, using Eqn. (5), the mass transfer coefficient h_m was found to be ≈ 20E-3 (m/s).

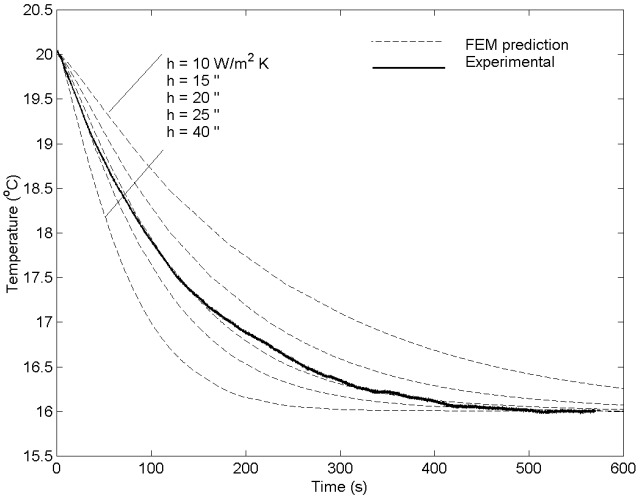

Figure 6. Experimental and FEM predictions of the temperature history in a specimen of cartilage during

4.6 Estimation of convective heat and mass transfer coefficients.

The temperature time history shown in Figure 6 (evaporative cooling effect) was used to estimate both heat and mass transfer coefficients. In the absence of irradiation, conservation of energy in a cartilage specimen in air reduces to a balance between latent energy lost by liquid evaporation and energy transfer to the liquid from the surrounding environment, which may be expressed as

$$h\ (T_\infty - T_s) = h_{fg}\, h_m [\rho_{vap,sat}(T_s) - \rho_{vap,\infty}] \qquad (7)$$

After thermal equilibrium is attained (t > 500 s), enough information is known (T_∞ = 23 °C, T_s = 16 °C, Rh = 50%) to determine a ratio between the heat and mass transfer coefficients, given as

$$\frac{h}{h_m} = \frac{h_{fg}\,[\rho_{vap,sat}(T_s) - \rho_{vap,\infty}]}{(T_\infty - T_s)} \qquad (8)$$

Equation (8) can then be substituted into Eqn. (1), with Q_i=0, and solved numerically using the finite element model to find the h value that matches best the experimental cooling history. Figure 6 shows a single experimental temperature-time curve along with several curves obtained using the FEM. The FEM predictions of temperature during water evaporation agreed very well with the experimental results when values of h in the 15-20 W/m^2 K range were used as input parameters in the

computer simulation. This range is in close agreement with typical values of h for free convection in gases, which range between 5-25 W/m^2 K [8]. Substituting h in Eqn. (8) gives values for the mass transfer coefficient h_m between 13E-3 and 17E-3 (m/s), which are in good agreement with those obtained in section 4.5.

5. RESULTS

5.1 Thermal response of cartilage: Model predictions.

Figure 7 shows the tissue response to laser irradiation as predicted by the FEM. The figure presents several isothermal contours showing the temperature distribution in a 2.3 mm thick cartilage specimen at the end of irradiation (t=10 s, P=5W). As expected, the FEM predicts higher temperatures at the center of the beam and at regions nearest to the irradiated surface (bottom surface in the model).

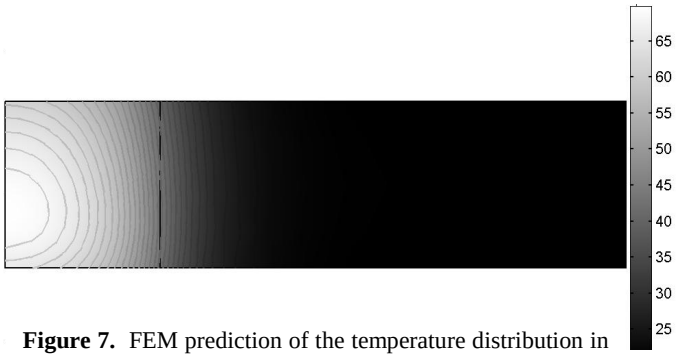

Figure 7. FEM prediction of the temperature distribution in a 2.3 mm thick cartilage at the end of laser irradiation (t=10 s. P=5 W).

Figure 8 presents the surface temperature history along the radius of the model ($0 < r < 10$mm) for the same specimen. It is clear from this figure that heating is a highly localized phenomenon almost limited to the laser target site, where significant temperature gradients develop. During irradiation the temperature rapidly increases to a value of 60 °C, followed by thermal relaxation when the laser is turned off until thermal equilibrium with the environment is reached.

Figure 9 illustrates temperature variation as a function of tissue depth, measured at the center of the laser irradiation site (r = 0). The calculation shown corresponds to a 2.3 mm thick specimen; at this tissue thickness the difference in temperature between front (z = 0 mm) and back (z = 2.3 mm) surfaces after laser irradiation (t=10 s) is about 5 °C. This difference becomes significant as thickness increases. For instance, if the specimen were 1 mm thicker (D = 3.3 mm), the difference would be close to 15 °C. The maximum temperature occurs inside the tissue ($z \cong 0.5$ mm) near the irradiated surface. This maximum temperature is about two degrees higher than that of the front surface.

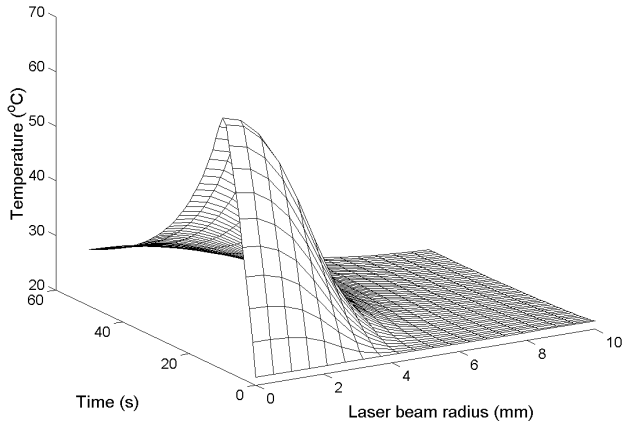

Figure 8. Surface temperature history of a 2.3 mm thick cartilage during and after laser irradiation (t=10 s, P=5 W).

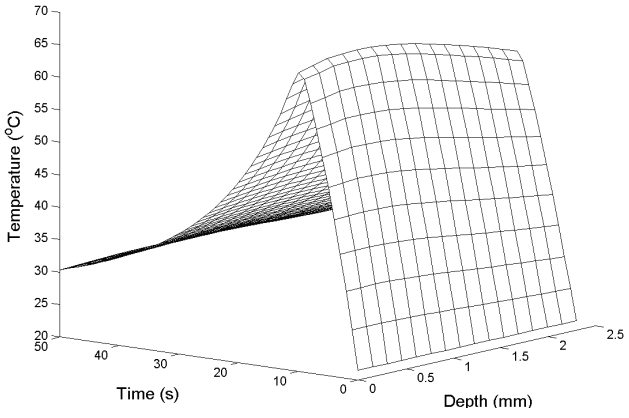

Figure 9. Temperature variation as a function of tissue depth at the center of the laser target site. Prediction made for a 2.3 mm thick cartilage during and after laser irradiation (t=10 s, P=5 W).

Figure 10 illustrates the temperature history of a point located at the tissue surface and at the center of the laser beam (z=0, r=0) when the cooling effect of evaporation is incorporated into the model. Values of *Rh* varying from dry (0%, maximum evaporation) to saturated air (100%, minimum evaporation) were used in the calculations. The figure also shows the temperature history as predicted by the model without water evaporation. Comparison among the curves reveals the importance of including water evaporation in the calculation of temperature. It can be seen that evaporation influences mainly the final temperature of the tissue, however, it also affects the heating rate and therefore the maximum temperature reached after laser irradiation, as shown in the inset in Figure 10.

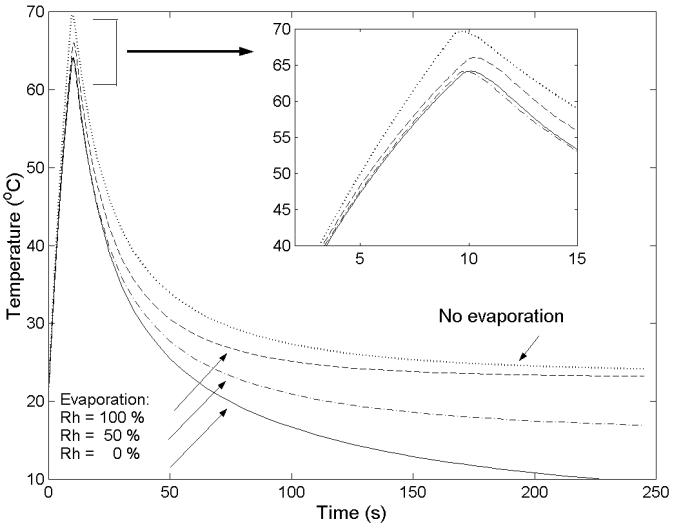

Figure 10. Surface temperature history of a 2.3 mm thick cartilage during and after laser irradiation (t=10 s, P=5 W). Comparison between calculations made for different environmental conditions.

5.2 Measurements and model predictions.

In Fig. 11, the surface temperatures predicted by the FEM are compared with temperatures measured experimentally during laser irradiation of a 2.3 mm thick cartilage specimen. The laser power was set at 5W while the irradiation time varied from 5 to 15 s. After each exposure, the specimen was immersed in saline solution for 10 min for re-hydration. In this comparison, the FEM temperatures correspond to the average surface temperatures of the region within a radius of 2 mm from the center of the irradiation site. The reason for doing this arithmetic mean is that the experimental measurement made with the infrared device is the average temperature of the entire surface within the field of view of the instrument, which is close to the detector aperture (r = 2.5 mm) at a sensor-to-object distance of 30 mm. Fig 11 shows good agreement between numerical and experimental results. The FEM predicts maximum temperatures at the end of the irradiation period well within a 10% error with respect to the experimental values. During thermal relaxation, the predicted curves deviate from the experimental results by showing higher cooling rates. This discrepancy might be due to localized cartilage dehydration after irradiation at regions near the beam spot. Theses reductions in water concentration results in lower water loss rates, which in turn affect the evaporative cooling.

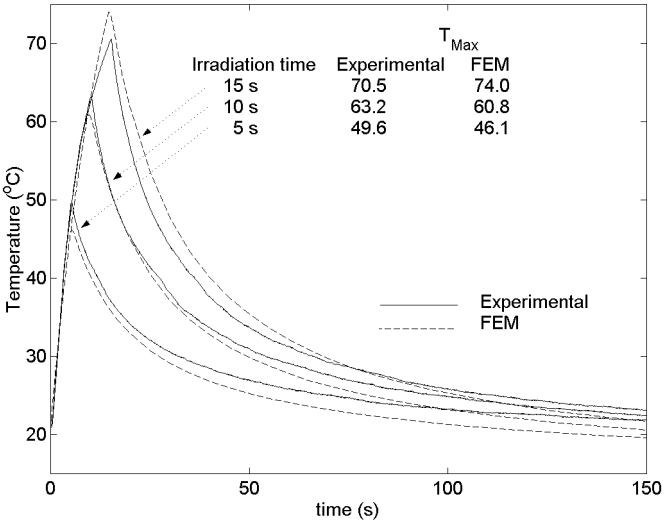

Figure 11. Surface temperature history of a 2.3 mm thick cartilage during and after laser irradiation (P=5 W). Comparison between experimental and FEM predictions for different irradiation times.

In Fig. 12, experimental and predicted surface temperatures of a 3.3 mm thick cartilage specimen are compared. In this case, the laser irradiation time was fixed at 5 s while varying the laser beam power from 6-10 W. As described above, the specimen was allowed to re-hydrate after each exposure. The surface temperatures predicted by the FEM show excellent agreement (within 5%) with experimental measurements. Fig. 13 also compares predicted and measured temperatures, but for a 0.95 mm thick cartilage specimen. Here as well, the laser irradiation time was fixed at 5 s and the laser beam powers used were 4-8 W. In contrast to the results shown in Fig 12, the FEM predictions for the 0.95 mm thick specimen overestimate (> 10%) the experimental temperature at the end of the irradiation when the laser parameters used led to surface temperatures above 50 °C. These discrepancies may be explained in terms of the tissue water concentration. A thin specimen should dehydrate faster than a thick one under the

same conditions, because the water volume per unit area in the former is lower. If we now postulate that light absorption (thermal energy deposition) depends on water concentration, then results from our FEM are more likely to deviate from experiments made on thinner specimens, since the model assumes constant water transfer rates from the tissue to the surroundings. Furthermore, water concentration in cartilage may influence both, convective heat and mass transfer coefficients, making both time and temperature dependent. However, our calculations assume that these coefficients remain constant.

5.3 Damage prediction.

Thermal damage is typically quantified using a single parameter, Ω, which is calculated from the Arrhenius integral formulation as

$$\Omega(\tau) = A\int_0^{\tau} e^{-\frac{E_a}{RT(t)}}dt \qquad (10)$$

where A (1/s) is a pre-exponential constant, τ (s) the total heating time , R (J/mole K) the universal gas constant, T (K) the absolute temperature, and E_a (J/mole) the activation energy of the transformation [13]. This form of damage integral has the advantage that it can be coupled to models of the temperature distribution in cartilage during laser irradiation to predict the onset, extent, and severity of thermal injury. As an example, Fig. 14 shows the extent of damage, Ω, predicted by the FE model in a 2.3 mm thick cartilage at the end of laser irradiation (t=10 s, P=5 W). The light and dark gray areas shown in Fig. 14 indicate regions where Ω < 1.0 and Ω > 2.0, respectively. In this simulation, $E_a = 4.5\text{x}10^5$ J/mole and $A = 8.3\text{x}10^{69}\text{s}^{-1}$ were used as the rate process coefficients representing thermal injury in cartilage. For tissue damage processes, A varies from about 10^{40} to 10^{105} s^{-1} while E_a ranges from 10^5 to 10^6 J/mole [13].

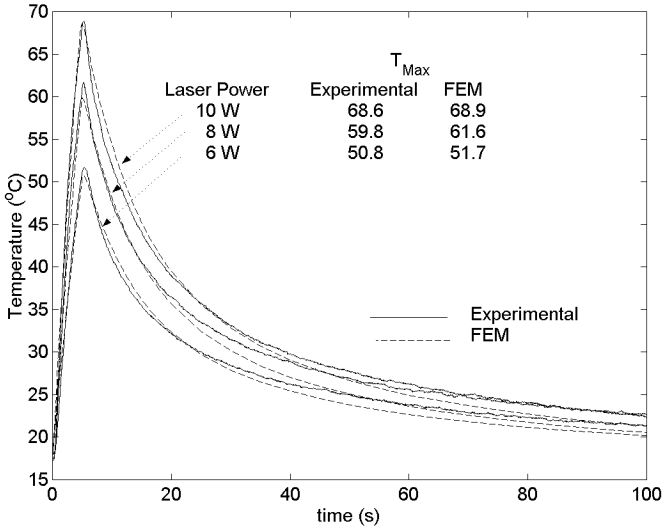

Figure 12. Surface temperature history of a 3.3 mm thick cartilage during and after laser irradiation (t = 5 s). Comparison between experimental and FEM predictions for different laser powers (6-10 W).

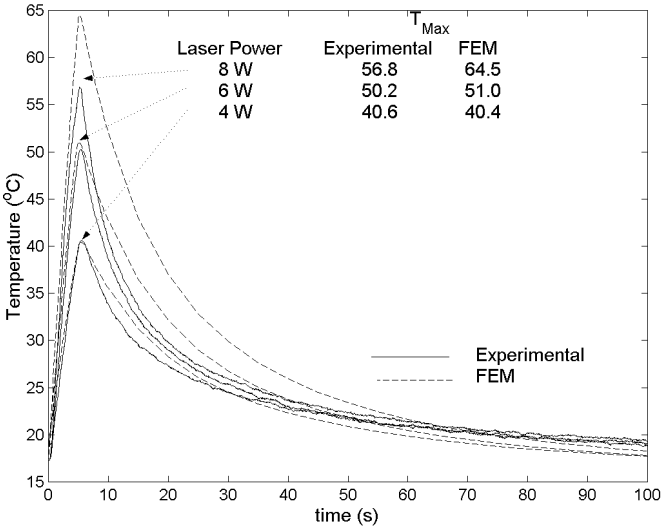

Figure 13. Surface temperature history of a 0.95 mm thick cartilage during and after laser irradiation (t = 5 s). Comparison between experimental and FEM predictions for different laser powers (4-8W).

6. DISCUSSION

In this study, we performed the experimental characterization of the thermal response of porcine cartilage that accompanies Nd:YAG (λ = 1.32 μm) laser irradiation. The surface temperature history was monitored during heating and thermal relaxation; using laser exposure times ranging between 1 and 15 s and laser powers of 1 to 10 W, which are parameters typically used for cartilage reshaping. The experimental results were then used to validate a FEM of the temperature response of laser-irradiated tissue. The numerical model accounts for heat diffusion, light propagation in tissue, and heat loss due to water evaporation. Due to its optical properties, photothermal heating of cartilage is a scattering dominated phenomenon. Hence, the photon density distribution in cartilage was estimated using a numerical solution of light propagation that included scattering. In addition to light interactions, the cooling effect of water evaporation at the tissue-air interface proved to have an important influence on the thermal response of cartilage. The experimental observations are supported by numerical results when vaporization is included in calculations of temperature. From the experimental results, heat and mass transfer coefficients were measured and found to be within the range of typical values for convective heat transfer in gases.

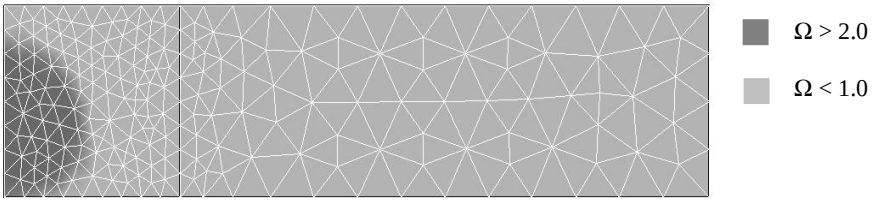

Figure 14. FEM prediction of thermal damage in a 2.3 mm thick cartilage at the end of laser irradiation (t=10 s, P=5 W). Light and dark gray areas indicate regions where $\Omega < 1.0$ and $\Omega > 2.0$, respectively.

The good agreement observed between FEM and experimental results are indicative that the major contributors determining the thermal response of cartilage to laser irradiation have been taken into account. Nevertheless, we are aware of the limitations of our approach, since several physical processes have been excluded from the FEM analysis. For instance, our model does not incorporate heat loss due to the low-energy phase transformations, which are known to take place in cartilage above a critical temperature $T_c \cong 65$ °C [3]. It is also known that the changing tissue optical properties alter the rate of energy deposition in tissue, thereby accelerating optical changes in some parts of the tissue [14]. Furthermore, temperature gradients in cartilage induce water transport across the tissue from irradiated to non-irradiated zones, which may in turn have a significant effect on the heat and mass transfer and light absorption coefficients. Therefore, a complete formulation of the thermal response of cartilage to laser heating should incorporate water mass transfer in bulk cartilage, which might in turn influence laser energy deposition rates and surface evaporation kinetics. We are currently addressing several of these issues.

7. CONCLUSION

The experimental work has led to the formulation and validation of the numerical model. The information rendered by the FEM will in turn, allow us to make predictions of: (a) the onset of new molecular arrangements in the material (phase change), which hypothetically are responsible of permanent shape change; and (b) estimation of thermal damage (denaturation) from the spatial and temporal temperature distribution using the so-called Arrhenius integral formulation (Pearce and Thomsen, 1995). By determining the thresholds and limits of both rate processes, a comprehensive relationship among the treatment parameters involved (time, tissue thickness, irradiance, etc.) will be established, thus conceiving the fundamental guidelines of laser cartilage thermoforming.

ACKNOWLEDGMENTS

This work was supported in part by the National Institutes of Health (AR43419 and DC 00170), Office of Naval Research (N00014-94-0874), Department of Energy (DE-FG03-91ER61227), and the Air Force Office of Scientific Research. The authors are grateful to Profs. J Stuart Nelson and Sam Tanenbaum for valuable discussions.

REFERENCES

[1] B. J. F. Wong, T.E. Milner, B. Anvari, A. Sviridov, A. Omel'chenko, V.V. Bagratashvili, E.N. Sobol, J.S. Nelson, "Measurement of radiometric surface temperature and integrated back-scattered light intensity during feedback controlled laser-assisted cartilage reshaping", *Lasers in Medical Science*, vol. 13, no. 1, pp. 66-72, 1998.

[2] Z. Wang, M.M. Pankratov, D.F. Perrault, S.M. Shapshay, "Laser-assisted cartilage reshaping: in vitro and in vivo animal studies", *Proc. SPIE*, vol. 2395, pp. 296-302, 1995.

[3] E.N. Sobol, A. Sviridov, V.V. Bagratashvili, A. Omel'chenko, Y.M. Ovchinnikov, A.B. Shekhter, V.M. Svistishkin, and A.N. Shinaev, "Laser reshaping of nasal septum cartilage: clinical results for 40 patients", *Proc. SPIE*, vol. 3907, pp. 297-302, May 2000.

[4] E.N. Sobol, *Phase transformations and ablation in laser-treated solids*, New York: John Wiley, pp. 316-322, 1995.

[5] C.S. Orr and R.C. Eberhart, "Overview of Bioheat transfer", in *Optical-Thermal Response of Laser-Irradiated Tissue*, A. J. Welsh and MJC van Gemert, eds. (Plenum, New York, 1995), pp 367-384.
[6] L.H. Wang, S.L. Jacques, and L.Q. Zheng, "MCML – Monte Carlo modeling of photon transport in multi-layered tissues", *Computer Methods and Programs in Biomedicine*, vol. 47, no. 2, pp. 131-146, 1995.
[7] L.H. Wang, S.L. Jacques, and L.Q. Zheng, "CONV – Convolution for responses to a finite diameter photon beam incident on multi-layered tissues", *Computer Methods and Programs in Biomedicine*, vol. 54, pp. 141-150, 1997.
[8] F.P. Incropera and D.P. DeWitt, *Fundamentals of Heat and Mass Tranfer* (Wiley, New York, 1996).
[9] B.J.F. Wong, K.K.H.Chao,H.K Kim, E.A. Chu, X. Dao, M.Gaon, C.H.Sun, and J.S. Nelson, "The porcine and lagomorph septal cartilages: Models for tissue engineering and morphologic cartilage research". *Amer. J. Rhinology*, vol. 15, no. 2, pp. 109-116, March 2000.
[10] S. Diaz, E. Lavernia, and B.J.F. Wong, "Mechanical behavior of cartilage during laser irradiation", *Proc. SPIE*, vol. 4257, pp. 192-197, 2001.
[11] S. Diaz, G. Aguilar, E. Lavernia, and B.J.F. Wong, "Modeling the thermal response of porcine cartilage to laser irradiation", *IEEE STQE*, vol. 7, No. 6, Nov-Dec 2001.
[12] J.I. Youn, S.A.Telenkov, E. Kim, N.C. Bahavaraju, B.J.F.Wong, J.W. Valvano, and T.E. Milner, "Optical and Thermal Properties of Nasal Septal Cartilage", *Lasers in Surgery and Medicine*, vol. 27, no. 2, pp 119-128, 2000. J.
[13] Pearce and S. Thomsen, "Rate process analysis of thermal damage", in *Optical-Thermal Response of Laser-Irradiated Tissue*, A. J. Welsh and MJC van Gemert, eds. (Plenum, New York, 1995), pp 561-606.
[14] S.L. Jacques, "Role of tissue optics and pulse duration on tissue effects during high-power laser irradiation", *Applied Optics*, vol. 32, no. 13, pp. 2447-2454, May 1993.